Research Article

MOLECULAR PAIN

Molecular Pain
Volume 19: 1–14

DOI: 10.1177/17448069231185439
journals.sagepub.com/home/mpx
Sage

BDNF-TrkB signaling pathway-mediated microglial activation induces neuronal KCC2 downregulation contributing to dynamic allodynia following spared nerve injury

Zihan Hu[1,*], Xinren Yu[1,*], Pei Chen[1,*], Keyu Jin[1], Jing Zhou[2,3], Guoxiang Wang[2], Jiangning Yu[2], Tong Wu[1], Yulong Wang[3], Fuqing Lin[1], Tingting Zhang[1], Yun Wang[2], and Xuan Zhao[1]

Abstract

Mechanical allodynia can be evoked by punctate pressure contact with the skin (punctate mechanical allodynia) and dynamic contact stimulation induced by gentle touching of the skin (dynamic mechanical allodynia). Dynamic allodynia is insensitive to morphine treatment and is transmitted through the spinal dorsal horn by a specific neuronal pathway, which is different from that for punctate allodynia, leading to difficulties in clinical treatment. K^+-Cl^- cotransporter-2 (KCC2) is one of the major determinants of inhibitory efficiency, and the inhibitory system in the spinal cord is important in the regulation of neuropathic pain. The aim of the current study was to determine whether neuronal KCC2 is involved in the induction of dynamic allodynia and to identify underlying spinal mechanisms involved in this process. Dynamic and punctate allodynia were assessed using either von Frey filaments or a paint brush in a spared nerve injury (SNI) mouse model. Our study discovered that the downregulated neuronal membrane KCC2 (mKCC2) in the spinal dorsal horn of SNI mice is closely associated with SNI-induced dynamic allodynia, as the prevention of KCC2 downregulation significantly suppressed the induction of dynamic allodynia. The over activation of microglia in the spinal dorsal horn after SNI was at least one of the triggers in SNI-induced mKCC2 reduction and dynamic allodynia, as these effects were blocked by the inhibition of microglial activation. Finally, the BDNF-TrkB pathway mediated by activated microglial affected SNI-induced dynamic allodynia through neuronal KCC2 downregulation. Overall, our findings revealed that activation of microglia through the BDNF-TrkB pathway affected neuronal KCC2 downregulation, contributing to dynamic allodynia induction in an SNI mouse model.

[1]Department of Anesthesiology, School of Medicine, Tongji University, Shanghai tenth People's Hospital, Shanghai, China
[2]Department of Neurology, Institutes of Brain Science, State Key Laboratory of Medical Neurobiology and MOE Frontiers Center for Brain Science, Zhongshan Hospital, Fudan University, Shanghai, China
[3]Rehabilitation Center, First Affiliated Hospital of Shenzhen University Health Science Center, Shenzhen Second People's Hospital, Shenzhen, China

*These authors contributed equally to this work

Corresponding Authors:
Tingting Zhang, Department of Anesthesiology, School of Medicine, Tongji University, Shanghai tenth People's Hospital, Shanghai 200072, China.
Email: ztt-sjtu@hotmail.com

Yun Wang, Department of Neurology, Institutes of Brain Science, State Key Laboratory of Medical Neurobiology and MOE Frontiers Center for Brain Science, Zhongshan Hospital, Fudan University, No. 131 Dongan Road, Xuhui District, Shanghai 200433, China.
Email: yunwang@fudan.edu.cn

Xuan Zhao, Department of Anesthesiology, School of Medicine, Tongji University, Shanghai tenth People's Hospital, Shanghai 200072, China.
Email: zhaoxuan301@tongji.edu.cn

Keywords
Dynamic allodynia, spared nerve injury, microglia, KCC2, BDNF-TrkB pathway

Date Received: 3 December 2022; Revised 2 May 2023; accepted: 16 May 2023

Introduction

Neuropathic pain is caused by disease or injury to the nervous system and includes various chronic conditions that affect up to 8% of the population.[1] There are two hallmarks of neuropathic pain: spontaneous pain and mechanical allodynia, which is a painful response to innocuous stimulus.[2] Mechanical allodynia occurs in multiple forms, including dynamic, punctate, and static. Dynamic allodynia is caused by gentle stimulation, such as that of garments on the skin, running water, or even wind, and is mediated by low-threshold mechanoreceptors. Punctate allodynia is evoked by stick or pin pricks and is signaled through thin unmyelinated C fibers and myelinated Aβ fibers. Static allodynia, which differs from punctate allodynia, is considered to be evoked by finger pressure applied to the skin or underlying tissue and is mediated by unmyelinated C fiber.[3,4] To date, the mechanisms underlying the distinct forms of mechanical allodynia, especially dynamic allodynia, remain unclear. Therefore, it is necessary to investigate the mechanism underlying dynamic mechanical allodynia to provide new treatment strategies.

The pain sensory system normally functions with a fine balance between excitation and inhibition. When this balance is perturbed, neuropathic pain develops. Based on accumulating evidence, this pain generation is attributed to specific dysfunctions of the inhibitory system in the spinal cord. One possible mechanism leading to the dysfunction of the inhibitory system is the downregulation of K + -Cl-cotransporter-2 (KCC2) expression, in which the alteration of KCC2 expression affects GABAergic and glycinergic neurotransmission, as KCC2 is a potassium chloride exporter that serves to maintain intracellular chloride concentration.[5] In fact, various neuropathic pain models have revealed a decrease in KCC2 expression in the spinal cord. A study using a rat model of peripheral nerve injury induced by implantation of a polyethylene cuff around the sciatic nerve was the first to demonstrate a relationship between neuropathic pain and downregulation of KCC2.[6] Subsequently, allodynia was observed in an animal model of diabetes induced by systemic streptozotocin administration, and a decrease in KCC2 expression in the spinal cord was noted.[7] These findings suggest that KCC2 downregulation in neurons is involved in chronic pain induced by nerve injury and inflammation. However, it is unknown whether dynamic pain, a subtype of mechanical neuropathic pain, is also related to altered KCC2 expression and function.

Spinal microglia activation in spared nerve injury (SNI) mice has been demonstrated to contribute to mechanical pain, including the dynamic form.[8] Therefore, signaling between microglia and neurons is essential for neuropathic pain transmission. Brain-derived neurotrophic factor (BDNF) has been found to alter the anion gradient and downregulate KCC2 expression by activating the tropomyosin-related kinase B (TrkB) receptor and its downstream signaling pathways, which has been suggested to be one of the mechanisms contributing to neuropathic pain.[9]

The transmission pathway of dynamic allodynia in the spinal dorsal horn differs from that of punctate allodynia, and it has also been reported to be insensitive to morphine treatment.[10] Thus, the aim of this study was to determine whether impairment of KCC2 after SNI is involved in the induction of dynamic allodynia and its underlying spinal mechanisms, which could further guide clinical treatment of dynamic pain.

Materials and methods

Animals

All animal studies and experimental procedures were approved by the Animal Care and Use Committee of the Shanghai 10th People's Hospital and Fudan University. Male C57BL/6J mice (6–8 weeks old) were purchased from Slac Laboratory Animal (Shanghai, China) and housed in the animal facilities of the Institute of Brain Science, Fudan University. The animal cages were kept under specific controlled conditions: room temperature (25 ± 1°C), humidity (65 – 70%), and a 12 h light–dark cycle (light: 07:00–19:00; dark: 19:00–07:00). The animals were granted free access to food and water. After allowing adaptation for 1 week in the animal cages, the animals were randomly allocated to the experimental and control groups, and were subjected to the operation and drug injections described in the subsequent sections. All behavioral experiments were performed during the light phase.

SNI surgery

The SNI model was established as previously reported.[8,10,11] Briefly, anesthesia was induced with isoflurane (0.2%), followed by a 1-cm skin incision to expose the femur thigh of the left. The left tibial and common peroneal branches of the sciatic nerve were then ligated and transected distally while the sural nerve was left intact. In sham controls, the sciatic nerve and its branches were exposed without ligation or transection. Following all procedures, mice were placed in the recovery cage and observed until they were fully ambulatory

and could freely consume food and water. All mice were handled gently to minimize or eliminated animal distress during the examination.

Drug application

Drug administration was performed 30 min after surgery. Furosemide (Fur; 30 nmol), 5-(3-Bromophenyl)-1,3-dihydro-2H-benzofuro[3,2-e]-1,4-diazepin-2-one (5BDBD; 30 nmol), staurosporine aglycone (K252a; 30 nmol), minocycline (Mino; 30 nmol), brain-derived neurotrophic factor (BDNF; 3 ng/10 μL), BDNF + Mino (3 ng/10 μL+ 30 nmol) were respectively injected into the spinal cavity by intrathecal injection. Either normal saline or DMSO was used as the vehicle control in different sets of animal groups. K252a, BDNF, 5BDBD, and Mino were purchased from Sigma-Aldrich (St Louis, MO, USA).

Mechanical pain behavior test

For 3 days prior to SNI surgery, all mice were placed on the apparatus for acclimate to the new environment. After habituation and baseline sensitivity measurements, mice were examined for both punctate and dynamic allodynia at consistent times of day for 3 days post-SNI surgery, with the test interval for punctate and dynamic allodynia being at least 15 min, as previously reported.[8,10,11]

Punctate allodynia. Von Frey filaments were used to measure the paw withdrawal threshold of experimental mice using the Dixon's up-down method.[12] Mice were placed on an elevated wire grid and the lateral plantar surface of the hindpaw was stimulated with calibrated von Frey monofilaments (0.02–1 g). Positive responses were identified via three lifts of five trials at 3-min intervals for each stimulus intensity.

Dynamic allodynia. The protocol used to evaluate dynamic allodynia was based on a previously published study.[13] Briefly, the operated left hindpaw was lightly stroked with a paint brush (10 hairs) from heel to toe. A scoring system was employed to determine the light-touch sensitivity of the mice. For each test, the scores were as follows: score 0 = walking away or occasional brief paw lifting (<1 s or less); score 1 = sustained lifting (>2 s) of the stimulated paw toward the body; score 2 = strong lateral lifting above the level of the body; score 3 = flinching or licking of the operated paw. The test was repeated three times at intervals of 10 s.

Tissue preparation

The experimental mice were transcardially perfused with 0.9% normal saline followed by 4% paraformaldehyde under anesthesia with chloral hydrate (SNI on day 3). The whole spinal cord was removed and post-fixed in 4% paraformaldehyde for 2 h and placed in 15% and 30% sucrose solution in 0.01 M phosphate-buffered saline (PBS) for dehydration, until submerged. Coronal lumbar spinal sections were cut into 30-mm by sections using a freezing microtome (Leica, Germany).

Immunohistochemistry

Spinal cord tissue sections were processed for visualization of Iba-1 and KCC2 protein expression by immunofluorescence labeling in the dorsal horn. The sections were incubated overnight at 4°C in PBS containing 10% donkey serum and a mixture of two antibodies: rabbit monoclonal anti-Iba-1 antibody (dilution 1:200, GeneTex, SAN Antonio, Texas, USA) and mouse polyclonal anti-KCC2 (dilution 1:300, Abcam, Boston, Massachusetts, USA). After thorough rinsing, the sections were incubated for 2 h at room temperature in a mixture of two corresponding secondary fluorescently tagged antibodies (dilution at 1:300, Alexa Fluor 488 for Iba-1, and KCC2: dilution at 1:500, Alexa Fluor 647 for Neun; Invitrogen, Carlsbad, California, USA). The sections were covered with glass coverslips and imaged using a fluorescence microscope (Olympus, Japan). The fluorescence intensities of the Iba-1 and KCC2 proteins in the spinal dorsal horn were analyzed using ImageJ software.

Western blots

Western blotting (WB) was performed as described previously.[11] Tissue lysates from the spinal dorsal horn were prepared using Homo buffer, and the samples were centrifuged at 2250 g for 15 min at 4°C. The supernatant was then collected, and the protein content was determined using the Pierce BCA Protein Assay Kit (Thermo Fisher Scientific Inc., Waltham, MA, USA) following the manufacturer's protocol. Proteins were separated on 8% or 12% SDS-PAGE gradient gels and transferred onto polyvinylidene fluoride (PVDF) transfer membrane. The membrane was then incubated with mouse anti-KCC2 (07-432; Merck, New Jersey, USA) and mouse anti-β-actin (66009; Proteintech, Chicago, IL, USA) antibodies at 4°C overnight. Appropriate secondary antibodies conjugated to HRP were used (Thermo Fisher Scientific Inc.), and ECL reagents (Thermo Fisher Scientific Inc.) were employed for immunodetection. Signals were measured using ImageJ software and presented as relative intensity versus control. β-Actin was used as an internal control to normalize the band intensity.

Statistical analysis

Normal distribution was determined using the Kolmogorov–Smirnov test, and the variance was compared. Unless otherwise stated, statistical significance was determined using one-way or two-way analysis of variance (ANOVA), followed by the Bonferroni post hoc test for multiple comparisons. Data were analyzed using GraphPad Prism (Version 9.0.X; GraphPad Software, Inc., La Jolla, CA, USA) and are

presented as mean ± SEM. Statistical significance was set at $p < 0.05$.

Results

SNI-induced KCC2 reduction in the spinal dorsal horn contributed to dynamic allodynia

SNI induces long-lasting ipsilateral mechanical allodynia.[14] Consistent with our previous studies,[8,11] SNI induced robust mechanical allodynia in mice, including both dynamic (sensitive to paint brush) and punctate (sensitive to von Frey filaments) allodynia, on the ipsilateral hind paw 1 day after SNI surgery, and lasted for at least 3 days (Figure 1(a) and (b)). Similar as previously reported, the KCC2 and membrane KCC2 (mKCC2) levels were then examined on day 3 in both the SNI and sham surgery groups by using immunofluorescence and WB experiments. Both KCC2 and mKCC2 expression in the spinal dorsal horn were significantly reduced by SNI surgery in comparison with the sham operation (Figure 1(c)–(f)). To further verify whether the downregulation of mKCC2 was at least one of the causing factors leading to SNI-induced dynamic allodynia, furosemide (Fur), a KCC2 inhibitor previously demonstrated to acutely prevent mKCC2 downregulation during convulsant stimulation,[15] was administered intrathecally (i.t.) 30 min after SNI surgery to inhibit the injury-induced acute loss of mKCC2. Fur (30 nmol, i.t.) significantly inhibited SNI-induced dynamic and punctate allodynia ($p < 0.001$), with a more profound effect on dynamic allodynia, particularly on days 2 and 3 after

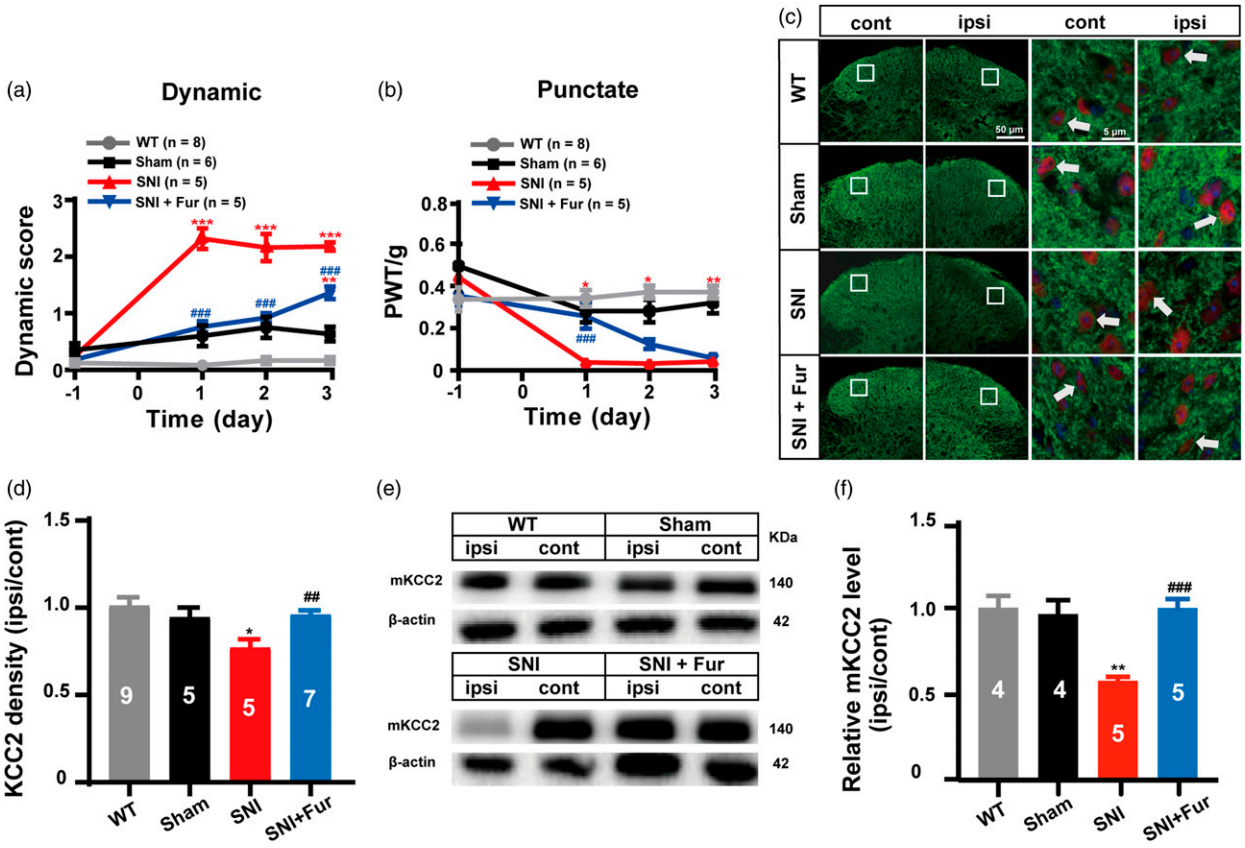

Figure 1. Neuronal membrane KCC2 downregulation in spinal dorsal horn partly mediated SNI-induced dynamic allodynia. (a) Furosemide (30 nmol, i.t.) treatment after SNI surgery prevented the induction of the dynamic allodynia. (WT, n = 8; Sham, n = 6; SNI, n = 5; SNI + Fur, n = 5; red $^{***}p < 0.001$, SNI group vs Sham group; blue $^{**}p < 0.01$, SNI + Fur group vs Sham group; blue $^{\#\#\#}p < 0.001$, SNI + Fur group vs SNI group, two-way ANOVA followed by Bonferroni post hoc analysis). (b) Treatment with furosemide (30 nmol, i.t.) prevented the induction of punctate allodynia at day 1 after SNI surgery. (WT, n = 8; Sham, n = 6; SNI, n = 5; SNI + Fur, n = 5; red $^{*}p < 0.05$, $^{**}p < 0.01$, SNI group vs Sham group; blue $^{*}p < 0.05$, SNI + Fur group vs Sham group; blue $^{\#\#\#}p < 0.001$, SNI + Fur group vs SNI group, two-way ANOVA followed by Bonferroni post hoc analysis). (c) Representative immunostaining images of KCC2 (green) and NeuN (red) in the spinal dorsal cord, arrows showing the likely neuron membrane KCC2. Scale bar, 50 μm (left), 5 μm (right). (d) The histograms respectively show the quantification of ratio of immunostaining KCC2 density on ipsilateral (ipsi) and contralateral (cont) sides of dorsal spinal cord after SNI surgery. (WT, n = 9; Sham, n = 5; SNI, n = 5; SNI + Fur, n = 7; $^{*}p < 0.05$, SNI group vs Sham group; $^{\#\#}p < 0.01$, SNI + Fur group vs SNI group, unpaired Student's t test). (e) Western blot of membrane KCC2 in the spinal dorsal cord. (f) The histograms respectively show the relative mKCC2 level on ipsilateral (ipsi) and contralateral (cont) sides of dorsal spinal cord after SNI surgery. (WT, n = 4; Sham, n = 4; SNI, n = 5; SNI + Fur, n = 5; $^{**}p < 0.01$, WT group, SNI group or SNI + Fur group vs Sham group; $^{\#\#\#}p < 0.001$, SNI + Fur group vs SNI group, unpaired Student's t test).

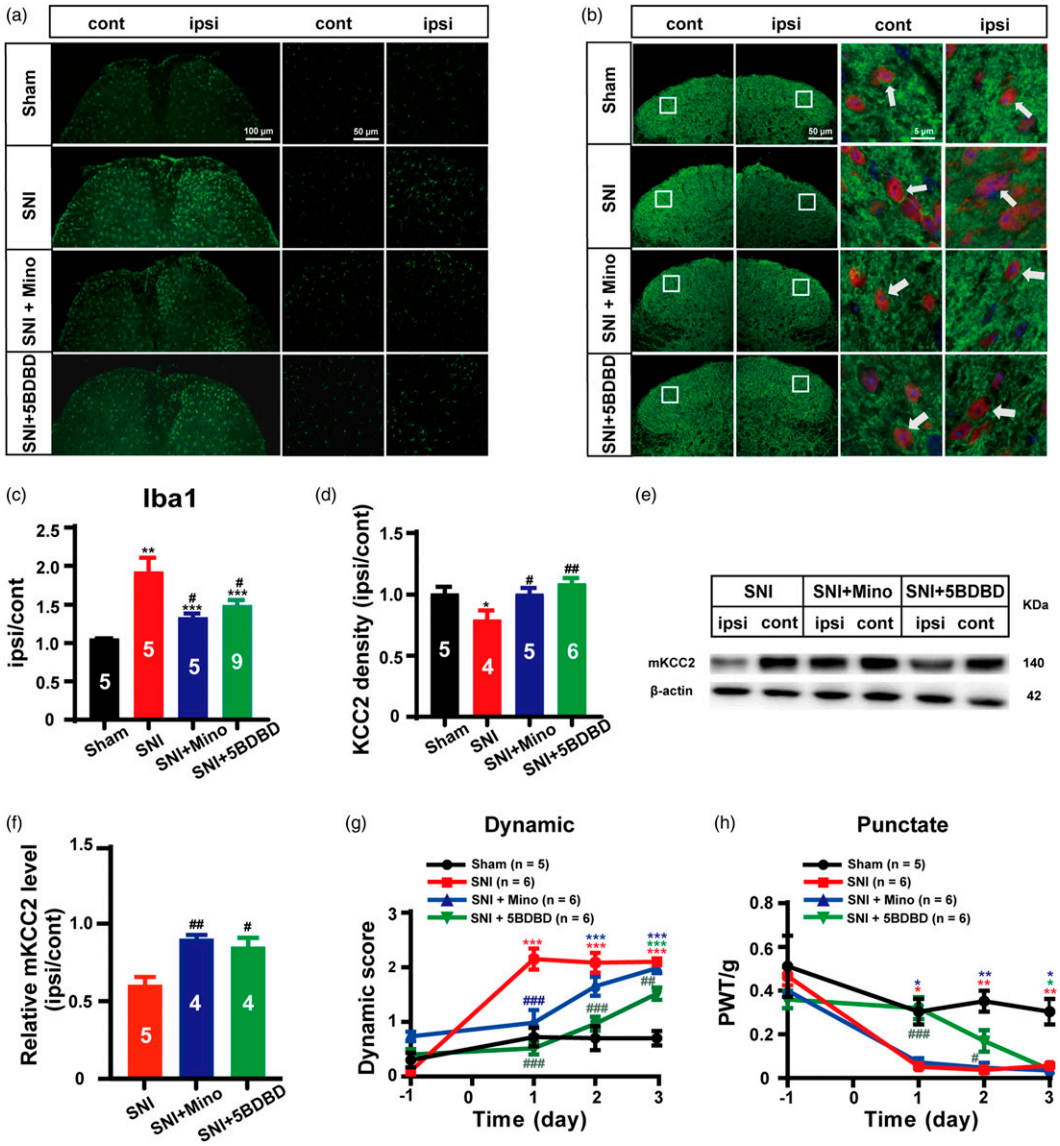

Figure 2. Activation of microglia in spine dorsal horn is involved in SNI induced mKCC2 reduction and dynamic allodynia. (a) Representative immunostaining images of microglia in the spinal dorsal. Scale bar, 100 μm (left), 50 μm (right). (b) Representative immunostaining images of KCC2 (green) and NeuN (red) in the spinal dorsal, arrows showing the likely neuron membrane KCC2. Scale bar, 50 μm (left), 5 μm (right). (c) The histograms respectively show the quantification of ratio of immunostaining density on ipsilateral (ipsi) and contralateral (cont) sides of dorsal spinal cord after SNI surgery. (Sham, n = 5; SNI, n = 5; SNI + Mino; n = 5; SNI + 5BDBD, n = 9, $^{**}p < 0.01$, SNI group vs Sham group, $^{***}p < 0.001$, SNI +Mino group or SNI +5BDBD group vs Sham group; $^{\#}p < 0.05$, SNI + 5BDBD group vs SNI group, $^{\#}p < 0.05$ SNI + Mino group vs SNI group, unpaired Student's t test). (d) The histograms respectively show the quantification of ratio of immunostaining KCC2 density on ipsilateral (ipsi) and contralateral (cont) sides of dorsal spinal cord after SNI surgery. (Sham, n = 5; SNI, n = 4; SNI + Mino; n = 5; SNI + 5BDBD, n = 6, $^{*}p < 0.05$, SNI group vs Sham group; $^{\#\#}p < 0.01$, SNI + 5BDBD group vs SNI group, $^{\#}p < 0.05$ SNI + Mino group vs SNI group, unpaired Student's t test). (e) Western blot of membrane KCC2 in the spinal dorsal cord. (f) The histograms respectively show the relative mKCC2 level on ipsilateral (ipsi) and contralateral (cont) sides of dorsal spinal cord after SNI surgery. (SNI, n = 5; SNI + Mino, n = 4; SNI + 5BDBD, n = 4; $^{\#}p < 0.05$, SNI + 5BDBD group vs SNI group, $^{\#\#}p < 0.01$, SNI + Mino group vs SNI group, unpaired Student's t test). (g) Minocycline (30 nmol, i.t.) or 5BDBD (30 nmol, i.t.) treatment after SNI surgery prevented the induction of the dynamic allodynia. (Sham, n = 5; SNI, n = 6; SNI + Mino, n = 6; SNI + 5BDBD, n = 6; red $^{***}p < 0.001$, SNI group vs Sham group; blue $^{***}p < 0.001$, SNI + Mino group vs Sham group; green $^{***}p < 0.001$, SNI + 5BDBD group vs Sham group; blue $^{\#\#\#}p < 0.001$, SNI + Mino group vs SNI group; green $^{\#\#}p < 0.01$, $^{\#\#\#}p < 0.001$ SNI + 5BDBD group vs SNI group; two-way ANOVA followed by Bonferroni post hoc analysis). (h) Minocycline (30 nmol, i.t.) treatment after SNI surgery had no effect on the punctate allodynia, but 5BDBD (30 nmol, i.t.) treatment after SNI surgery prevented the induction of punctate allodynia at day 1 and day 2. (Sham, n = 5; SNI, n = 6; SNI + Mino, n = 6; SNI + 5BDBD, n = 6; red $^{*}p < 0.05$, $^{**}p < 0.01$, SNI group vs Sham group; blue $^{*}p < 0.05$, $^{**}p < 0.01$, SNI + Mino group vs Sham group; green $^{*}p < 0.05$, SNI + 5BDBD group vs Sham group; green $^{\#}p < 0.05$, $^{\#\#\#}p < 0.001$ SNI + 5BDBD group vs SNI group; two-way ANOVA followed by Bonferroni post hoc analysis).\

SNI surgery (Figure 1(a) and (b)). Fur (30 nmol, i.t.) significantly inhibited the decrease in KCC2 expression in the spinal dorsal horn (Figure 1(c)), particularly the downregulation of KCC2 density in spinal dorsal horn neurons induced by SNI (Figure 1(d)). As depicted in Figure 1(c) and (d), the sham group had no change in the immunofluorescence intensity of KCC2, whereas the SNI group showed a significant reduction in the intensity in the ipsilateral spinal dorsal horn after SNI surgery ($p = 0.0465$). Fur significantly inhibited the loss of KCC2 immunofluorescence intensity induced by SNI surgery ($p = 0.0036$). In addition, the WB experimental results showed that the mKCC2 expression level in the ipsilateral dorsal horn was significantly decreased in the SNI group compared with that in the Sham group (SNI vs. Sham, $p = 0.0013$; Figure 1(e) and (f)). Similar to the immunofluorescence result, Fur was found to significantly inhibit the downregulation of KCC2 expression (SNI + Fur vs. SNI, $p < 0.001$; Figure 1(e) and (f)) to a level almost similar to that of the WT group. These experimental results indicate that the induction of dynamic allodynia by SNI is likely associated with a significant downregulation of mKCC2 levels in the spinal dorsal horn.

SNI-induced dynamic allodynia associated with microglia activation in the spinal dorsal horn caused neuronal mKCC2 reduction

The activation of microglia in the spinal dorsal horn in response to peripheral nerve injury is important in the development of neuropathic pain.[16] Previously we demonstrated that the inhibition of microglial activation could suppress SNI-induced dynamic allodynia.[8] Thus, we performed experiments to investigate whether SNI-induced microglia activation in the spinal dorsal horn is related to the downregulation of neuronal mKCC2, which further leads to the induction of dynamic allodynia. Mino (30 nmol), a non-specific P38 MAP kinase blocker, has been used as an effective microglial inhibitor,[17] which has been previously shown to inhibit dynamic allodynia in an SNI mice model.[8] In addition, as the P2X4 purinergic receptor has been known to mediate nerve injury-evoked microglial activation, 5-(3-bromophenyl)-1,3-dihydro-2H-benzofuro [3,2-e]-1,4-diazepin-2-one (5BDBD), a P2X4 purinergic receptor antagonist,[18] was also applied to block SNI-induced microglial activation in the spinal dorsal horn in the current study. Under our experimental conditions, similar to previous assessments, significant SNI-induced microglial activation was observed (SNI vs. Sham, $p = 0.0014$; Figure 2(a) and (c)); however, the administration of either Mino (30 nmol, i.t.) or 5BDBD (30 nmol, i.t.) 30 min after SNI surgery significantly inhibited spinal dorsal horn microglia activation (SNI + Mino vs. SNI, $p = 0.0135$; SNI + 5BDBD vs. SNI, $p = 0.0181$; Figure 2(a) and (c)). Under these conditions, KCC2 levels in the spinal dorsal horn were analyzed using immunofluorescence and WB. Based on the same immunohistochemistry experimental samples, both Mino and 5BDBD significantly reversed SNI-induced KCC2 expression levels (SNI + Mino vs. SNI, $p = 0.0350$; SNI + 5BDBD vs. SNI, $p = 0.0066$; Figure 2(b) and (d)) in the spinal dorsal horn. Similarly, the WB results from another set of animals confirmed that both Mino and 5BDBD significantly inhibited SNI-induced spinal dorsal horn mKCC2 expression (SNI + Mino vs. SNI, $p = 0.0016$; SNI + 5BDBD vs. SNI, $p = 0.0128$; Figure 2(e) and (f)). These data indicate that the inhibition of SNI-induced microglial activation could effectively block spinal dorsal horn neuronal KCC2 downregulation.

We further determined the effect of microglial inhibition on SNI-induced pain sensation. As expected, our behavioral data revealed that both Mino and 5BDBD significantly suppressed SNI-induced dynamic allodynia, but had less effect on punctate allodynia in our SNI mouse model. As shown in Figure 2(g), Mino significantly inhibited the induction of dynamic allodynia on day 1 ($p < 0.001$), but induced no significant changes on day 2 ($p = 0.1755$) and day 3 ($p = 0.9701$) after SNI surgery compared with that observed in the SNI group. Punctate allodynia did not significantly change in the Mino treatment group after SNI (SNI + Mino vs. SNI, $p > 0.05$; Figure 2(h)). Further, 5BDBD significantly inhibited the induction of dynamic allodynia during the 2-day testing period ($p < 0.001$; Figure 2(g)) and the third day ($p = 0.0099$; Figure 2(g)). In contrast, punctate allodynia was suppressed on day 1 ($p < 0.001$) and day 2 ($p = 0.0255$), but not on day 3 ($p > 0.05$), after SNI surgery compared with that found in the SNI group (Figure 2(h)).

In conclusion, the activation of microglial cells after SNI injury likely contributed to the downregulation of neuronal mKCC2 and the selective induction of dynamic allodynia.

The BDNF-TrkB signaling pathway mediates microglia activation-induced neuronal KCC2 downregulation and dynamic allodynia in mice with SNI

BDNF acting on its receptor tropomyosin-related kinase B (TrkB) to activate its internal signaling pathway is reported to phosphorylate KCC2 and cause the downregulation of mKCC2 expression.[19] Thus, we opted to determine whether SNI-induced microglial activation, KCC2 downregulation, and subsequent dynamic allodynia were mediated by the activation of the BDNF-TrkB pathway. For this determination, K252a, a potent inhibitor of receptor tyrosine kinases of the Trk family,[20] was administered intrathecally 30 min after SNI surgery. Immunohistochemistry and WB were used to verify either the microglia or mKCC2 level in the spinal dorsal horn on day 3 after SNI. Indeed, our immunohistochemistry results revealed that K252a (30 nmol, i.t.) significantly suppressed the loss of the KCC2 immunofluorescence signal (SNI + K252a vs. SNI, $p = 0.0343$; SNI + K252a vs. Sham, $p = 0.3229$; Figure 3(b) and (d)) induced by SNI, but had no effect on SNI-induced

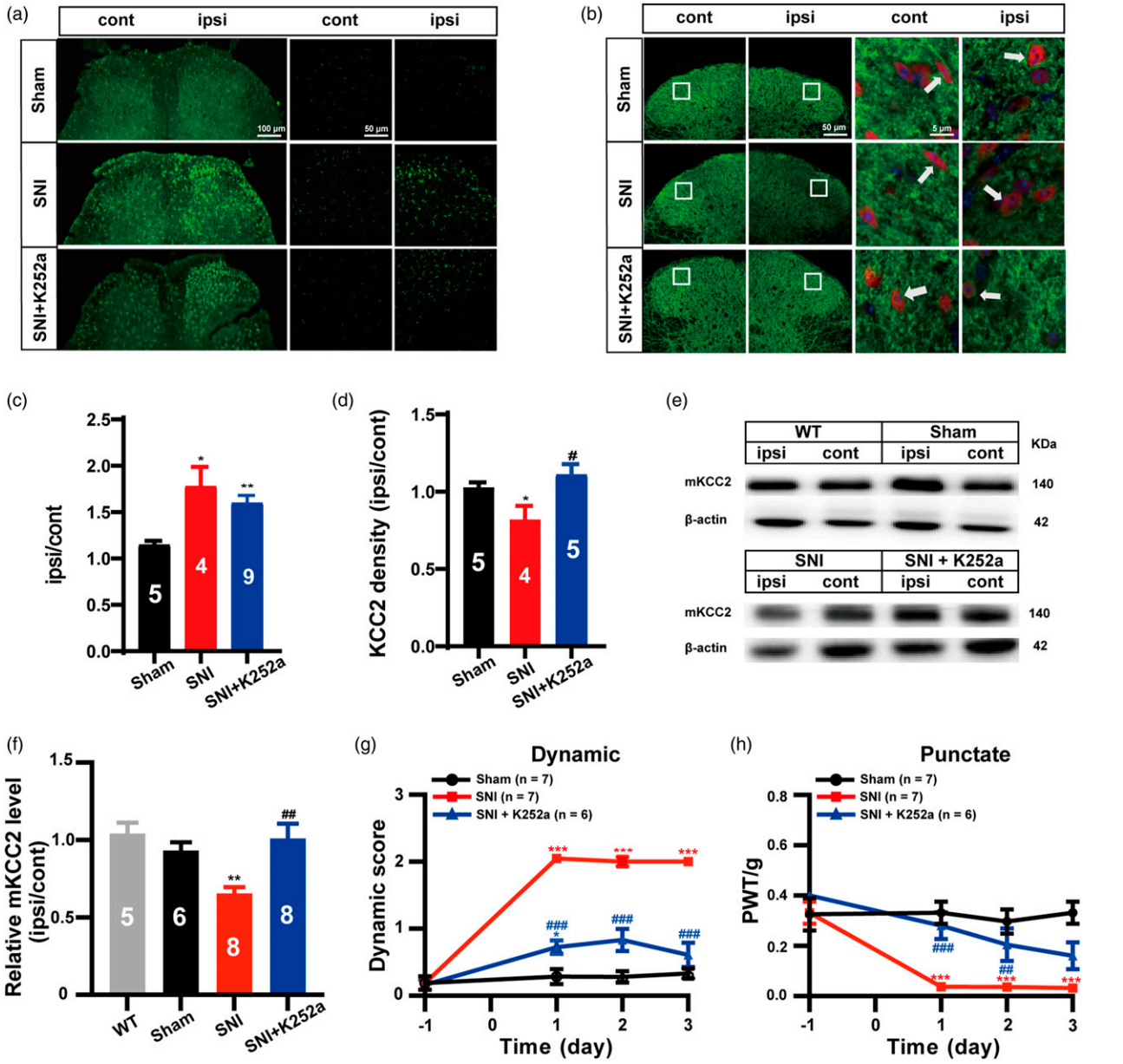

Figure 3. Activation of spinal dorsal horn microglia triggered BDNF-TrkB pathway induced neuronal KCC2 down regulation contributes to the dynamic allodynia in SNI mice. (a) Representative immunostaining images of microglia in the spinal dorsal. Scale bar, 100 μm (left), 50 μm (right). (b) Representative immunostaining images of KCC2 (green) and NeuN (red) in the spinal dorsal, arrows showing the likely neuron membrane KCC2. Scale bar, 50 μm (left), 5 μm (right). (c) The histograms respectively show the quantification of ratio of immunostaining density on ipsilateral (ipsi) and contralateral (cont) sides of dorsal spinal cord after SNI surgery. (Sham, n = 5; SNI, n = 4; SNI + K252a, n = 9; $^{*}p < 0.05$, $^{**}p < 0.01$, SNI group or SNI +K252a group vs Sham group; unpaired Student's t test). (d) The histograms respectively show the quantification of ratio of immunostaining KCC2 density on ipsilateral (ipsi) and contralateral (cont) sides of dorsal spinal cord after SNI surgery. (Sham, n = 5; SNI, n = 4; SNI + K252a, n = 5; $^{*}p < 0.05$, SNI group vs Sham group; $^{\#}p < 0.05$, SNI + K252a group vs SNI group, unpaired Student's t test). (e) Western blot of membrane KCC2 in the spinal dorsal cord. (f) The histograms respectively show the relative mKCC2 level on ipsilateral (ipsi) and contralateral (cont) sides of dorsal spinal cord after SNI surgery. (WT, n = 5; Sham, n = 6; SNI, n = 8; SNI + K252a, n = 8; $^{**}p < 0.01$, SNI group vs Sham group, $^{\#\#}p < 0.01$, SNI + K252a group vs SNI group, unpaired Student's t test). (g) K252a (30 nmol, i.t.) treatment after SNI surgery prevented the induction of the dynamic allodynia. (Sham, n = 7; SNI, n = 7; SNI + K252a, n = 6; red $^{***}p < 0.001$, SNI group vs Sham group; blue $^{*}p < 0.05$, SNI + K252a group vs Sham group; blue $^{\#\#\#}p < 0.001$, SNI + K252a vs SNI group; two-way ANOVA followed by Bonferroni post hoc analysis). (h) K252a (30 nmol, i.t.) treatment after SNI surgery prevented the induction of the punctate allodynia. (Sham, n = 7; SNI, n = 7; SNI + K252a, n = 6; red $^{***}p < 0.001$, SNI group vs Sham group; blue $^{\#\#}p < 0.01$, $^{\#\#\#}p < 0.001$, SNI + K252a group vs SNI group; two-way ANOVA followed by Bonferroni post hoc analysis).

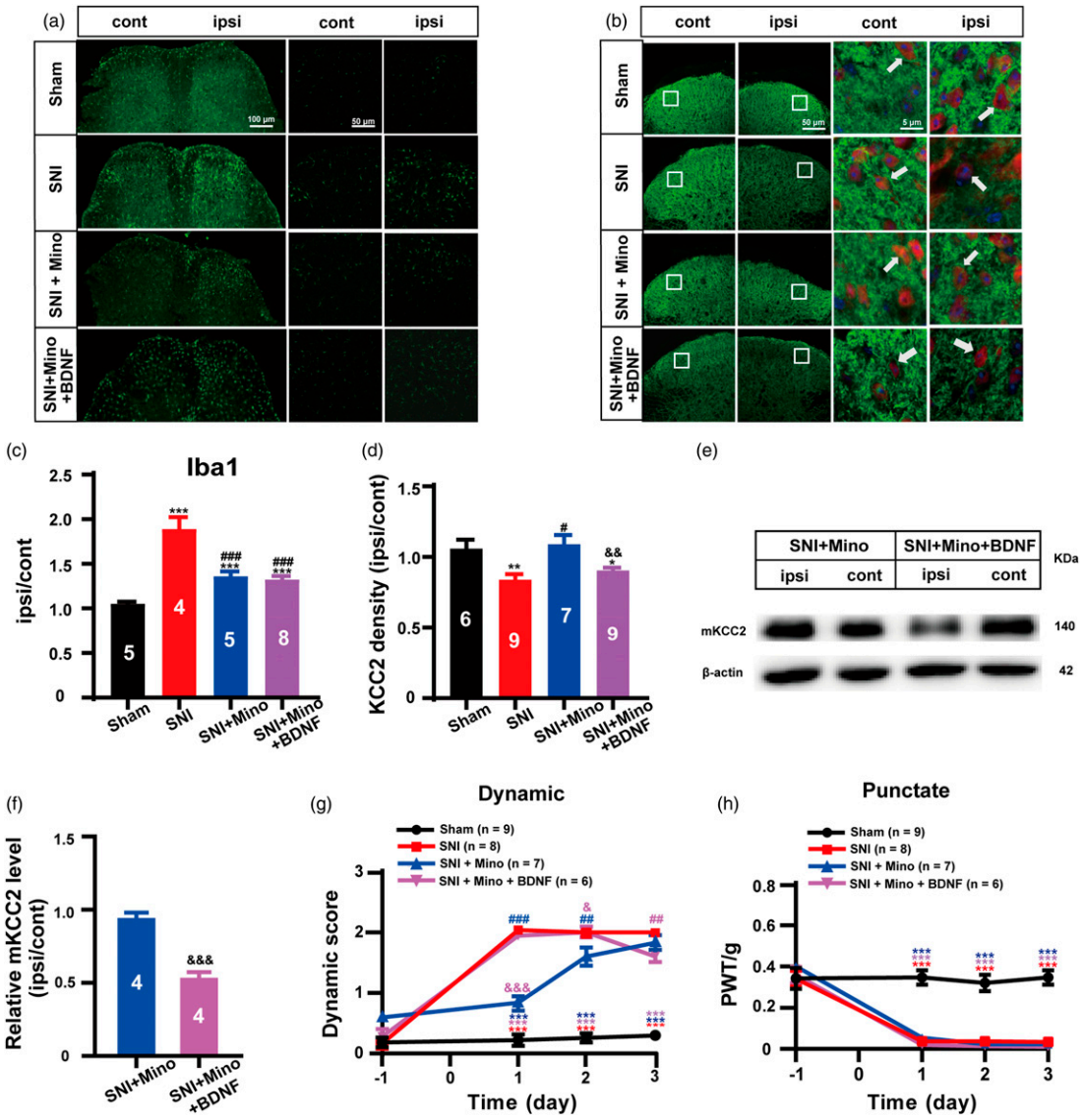

Figure 4. BDNF treatment reversed anti-glia activation to induce dynamic allodynia through mKCC2 down regulation. (a) Representative immunostaining images of microglia in the spinal dorsal. Scale bar, 100 μm (left), 50 μm (right). (b) Representative immunostaining images of KCC2 (green) and NeuN (red) in the spinal dorsal, arrows showing the likely neuron membrane KCC2. Scale bar, 50 μm (left), 5 μm (right). (c) The histograms respectively show the quantification of ratio of immunostaining density on ipsilateral (ipsi) and contralateral (cont) sides of dorsal spinal cord after SNI surgery. (Sham, n = 5; SNI, n = 4; SNI + Mino, n = 5; SNI + Mino + BDNF, n = 8; $^{***}p < 0.001$, SNI group, SNI + Mino group or SNI + Mino + BDNF group vs Sham group; $^{\#\#\#}p < 0.01$, SNI + Mino group vs SNI group; $^{\#\#\#\#}p < 0.001$, SNI + Mino + BDNF group vs SNI group; unpaired Student's t test). (d) The histograms respectively show the quantification of ratio of immunostaining KCC2 density on ipsilateral (ipsi) and contralateral (cont) sides of dorsal spinal cord after SNI surgery. (Sham, n = 6; SNI, n = 9; SNI + Mino, n = 7; SNI + Mino + BDNF, n = 9; $^{*}p < 0.05$, SNI + Mino + BDNF group vs Sham group, $^{**}p < 0.01$, SNI group vs Sham group; $^{\#\#}p < 0.01$, SNI + Mino group vs SNI group; &&$p < 0.01$, SNI + Mino + BDNF group vs SNI + Mino group; unpaired Student's t test). (e) Western blot of membrane KCC2 in the spinal dorsal cord. (f) The histograms respectively show the relative mKCC2 level on ipsilateral (ipsi) and contralateral (cont) sides of dorsal spinal cord after SNI surgery. (SNI + Mino, n = 4; SNI + Mino + BDNF, n = 4; &&&$p < 0.001$, SNI + Mino + BDNF group vs SNI + Mino group; unpaired Student's t test). (g) BDNF (3 ng/10 uL, i.t.), once a day for consecutive 2 days after SNI surgery with the Mino (30 nmol, i.t.) or the vehicle co-injected on the 1st day significantly reversed the blockade effect of Mino on SNI-induced dynamic allodynia on both day 1 and day 2. (Sham, n = 9; SNI, n = 8; SNI + Mino, n = 7; SNI + Mino + BDNF, n = 6; red $^{***}p < 0.001$, SNI group vs Sham group; blue $^{***}p < 0.001$, SNI + Mino group vs Sham group; purple $^{***}p < 0.001$, SNI + Mino + BDNF group vs Sham group; blue $^{\#\#}p < 0.01$, $^{\#\#\#}p < 0.001$, SNI + Mino group vs SNI group; purple $^{\#\#}p < 0.01$, SNI + Mino + BDNF group vs SNI group; purple &P < 0.05, &&&$p < 0.001$, SNI + Mino + BDNF group vs SNI + Mino group; two-way ANOVA followed by Bonferroni post hoc analysis). (h) BDNF (3 ng/10 uL, i.t.), once a day for consecutive 2 days after SNI surgery with the Mino (30 nmol, i.t.) or the vehicle co[1]injected on the 1st day had no effect on the punctate allodynia. (Sham, n = 9; SNI, n = 8; SNI + Mino, n = 7; SNI + Mino + BDNF, n = 6; red $^{***}p < 0.001$, SNI group vs Sham group; blue $^{***}p < 0.001$, SNI + Mino group vs Sham group; purple $^{***}p < 0.001$, SNI + Mino + BDNF group vs Sham group; two-way ANOVA followed by Bonferroni post hoc analysis).

microglial activation (SNI + K252a vs. Sham, $p = 0.0020$; SNI + K252a vs. SNI, $p = 0.3470$; Figure 3(a) and (c)). The WB results further demonstrated that K252a significantly inhibited SNI-induced cell membrane KCC2 downregulation in the spinal dorsal horn (SNI + K252a vs. SNI, $p = 0.0037$; SNI + K252a vs. Sham, $p = 0.5169$; Figure 3(e) and (f)). Furthermore, as expected, our behavioral study showed that K252a (30 nmol, i.t.) significantly inhibited SNI-induced dynamic allodynia during the first 3-days testing period (SNI + K252a vs. SNI, $p < 0.001$; Figure 3(g)), as well as punctate allodynia (SNI + K252a vs. SNI, $p < 0.001$ on day 1; $p < 0.01$ on day 2, Figure 3(h)).

These results confirmed our hypothesis that the BDNF-TrkB signaling pathway-mediated microglia activation-induced neuronal KCC2 downregulation contributes to dynamic allodynia in an SNI mice model.

BDNF is highly involved in SNI-induced dynamic and punctate allodynia through KCC2 downregulation

As the BDNF-TrkB signaling pathway is an important mediator of SNI-induced KCC2 downregulation and dynamic allodynia, we further determined whether exogenous application of BDNF could overcome the blockade effect of microglia inhibitors on both KCC2 expression and dynamic allodynia. Our immunohistochemistry results showed that the administration of BDNF (3 ng/10 μL, i.t.), once per day for two consecutive days after SNI surgery with Mino (30 nmol, i.t.) or the vehicle co-injected on the first day, significantly reversed the blockade effect of Mino on SNI-induced KCC2 immunofluorescence intensity, resulting in a decrease to a level similar to that of the SNI group (SNI + Mino + BDNF vs. SNI + Mino, $p = 0.0086$; SNI + Mino + BDNF vs. SNI, $p = 0.1645$; Figure 4(b) and (d)), but there was no action on the suppressive effect of Mino on SNI-induced microglia activation (SNI + Mino + BDNF vs. SNI + Mino, $p = 0.5847$; Figure 4(a) and (c)). Similarly, our WB results showed that BDNF alone not only evoked mKCC2 downregulation in sham animals (Sham + BDNF vs. Sham, $p < 0.001$; Figure 5(a) and (b)), but also reversed Mino inhibition of SNI-induced mKCC2 downregulation (SNI + Mino + BDNF vs. SNI + Mino, $p < 0.001$; Figure 4(e) and (f)). As expected, BDNF (3 ng/10 μL, i.t.) significantly reversed the blockade effect of Mino on SNI-induced dynamic allodynia (SNI + Mino + BDNF vs. SNI + Mino, $p < 0.001$ on day 1; $p = 0.0393$ on day 2; Figure 4(g)), in our behavioral study, but had no effect on punctate allodynia ($p > 0.05$; Figure 4(h)).

In addition, our WB results showed that BDNF alone evoked mKCC2 downregulation in sham animals (Sham + BDNF vs. Sham, $p < 0.001$; Figure 5(a) and (b)), but BDNF

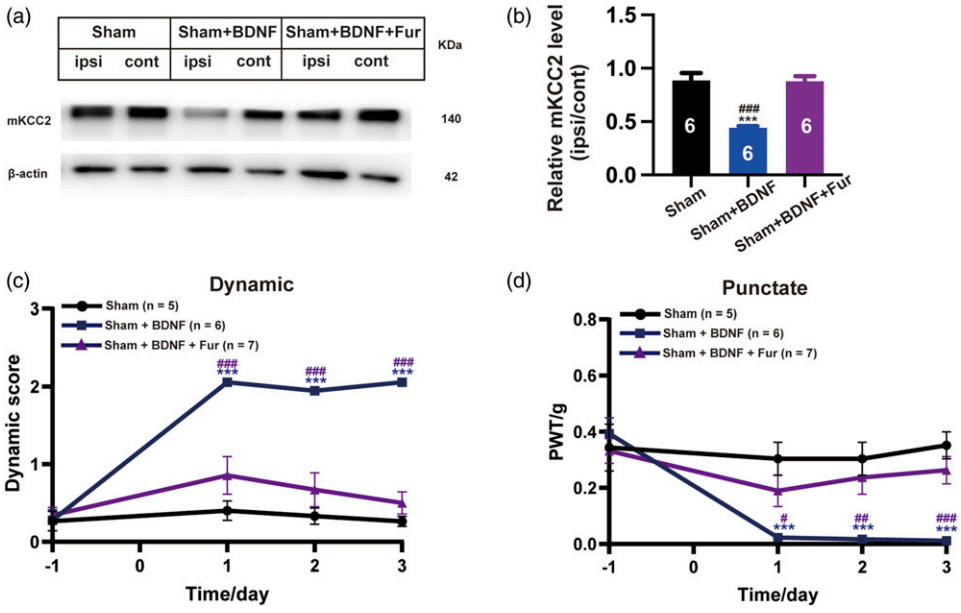

Figure 5. The involvement of KCC2 downregulation in BDNF-induced both dynamic and punctate allodynia. (a) Western blot of membrane KCC2 in the spinal dorsal cord. (b) The histograms respectively show the relative mKCC2 level on ipsilateral (ipsi) and contralateral (cont) sides of dorsal spinal cord (Sham, n = 6; Sham + BDNF, n = 6; Sham + BDNF +Fur, n = 6; $^{***}p < 0.001$, Sham group vs Sham + BDNF group; $^{\#\#\#}P < 0.001$, Sham + BDNF group vs Sham + BDNF +Fur group, unpaired Student's t test). (c) BDNF (3 ng/10 uL, i.t.) with the Fur (30 nmol, i.t.) co-injected on the 1st daysignificantly reversed the BDNF (3 ng/10 uL, i.t.) treatment alone evoked the dynamic allodynia. (Sham, n = 5; Sham + BDNF, n = 6; Sham + BDNF + Fur, n = 7; blue $^{***}p < 0.001$, Sham + BDNF vs Sham group; purple $^{\#\#\#}P < 0.001$, Sham + BDNF + Fur vs Sham + BDNF group, two-way ANOVA followed by Bonferroni post hoc analysis). (d) BDNF (3 ng/10 uL, i.t.) with the Fur (30 nmol, i.t.) co-injected on the 1st day significantly reversed the BDNF (3 ng/10 uL, i.t.) treatment alone evoked the punctate allodynia. (Sham, n = 5; Sham + BDNF, n = 6; Sham + BDNF + Fur, n = 7; blue $^{***}p < 0.001$, Sham + BDNF vs Sham group; purple $^{\#}p < 0.05$, $^{\#\#\#}p < 0.01$, $^{\#\#\#}p < 0.001$, Sham + BDNF + Fur vs Sham + BDNF group, two-way ANOVA followed by Bonferroni post hoc analysis).

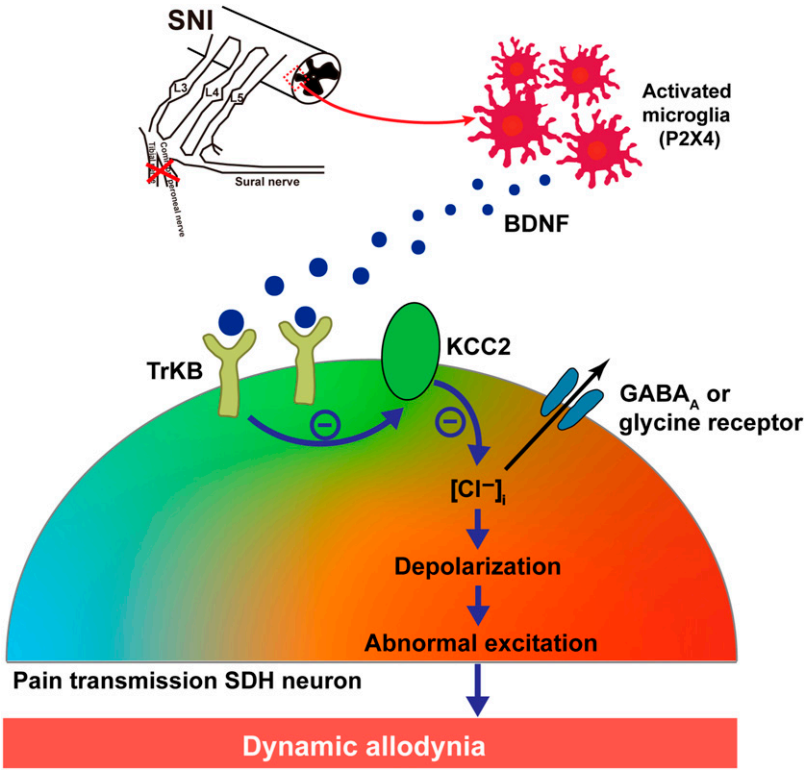

Figure 6. Scematic diagram of KCC2 contributing to dynamic allodynia. SNI activates spinal dorsal horn (SDH) microglia, which leads to the release of BDNF. BDNF downregulates KCC2 in SDH pain transmission neurons by combing with TrkB, causing an increase in intracellular Cl− and leading to a depolarizing shift in the anion reversal potential. The resulting hyperexcitability of pain transmission in neurons contributes to dynamic allodynia.

(3 ng/10 μL, i.t.) with Fur (30 nmol, i.t.) co-injected on the first day significantly reversed the BDNF (3 ng/10 μL, i.t.) alone treatment (Sham + BDNF + Fur vs. Sham + BDNF, $p < 0.001$; Figure 5(a) and (b)). This may imply that Fur could by preventing mKCC2 downregulation, reversing BDNF induced allodynia. The behavioral study also showed that BDNF (3 ng/10 μL, i.t.) significantly led to dynamic allodynia (Sham + BDNF vs. Sham, $p < 0.001$, Figure 5(c)), as well as punctate allodynia (Sham + BDNF vs. Sham, $p < 0.001$, Figure 5(d)) during the first 3-days testing period. However, BDNF (3 ng/10 μL, i.t.) with Fur (30 nmol, i.t.) co-injected on the first day significantly reversed the BDNF (3 ng/10 μL, i.t.) treatment alone evoking both dynamic allodynia (Sham + BDNF + Fur vs. Sham + BDNF, $p < 0.001$; Figure 5(c)) and punctate allodynia (Sham + BDNF + Fur vs. Sham + BDNF, $p = 0.0423$ on day 1; $p = 0.0043$ on day 2; $p = 0.0010$ on day 3; Figure 5(d)). Thus, these reversal experimental results further indicate that BDNF is an important mediating factor in SNI-induced dynamic allodynia through neuronal mKCC2 downregulation.

Discussion

Based on our results, SNI-induced dynamic allodynia is closely related to the downregulation of KCC2 through the BDNF-TrkB signaling pathway after SNI-induced microglial activation in the spinal dorsal horn (Figure 6). Furthermore, dynamic allodynia is more sensitive to SNI induced microglia-BNDF-TrkB-mKCC2 pathway dysfunction than punctate allodynia. This finding is based on the observation that (1) SNI induced both punctate and dynamic allodynia as well as the downregulation of neuronal mKCC2 in the spinal dorsal horn of mice, and the blockade of mKCC2 downregulation more profoundly reversed dynamic allodynia versus punctate allodynia. (2) Inhibition of SNI-induced spinal dorsal horn microglia activation prevented the downregulation of mKCC2 in spinal dorsal horn neurons and in turn blocked the development of SNI-induced dynamic allodynia with minor effects on punctate allodynia. (3) Blockade of the BDNF-TrkB signaling pathway suppressed mKCC2 downregulation and dynamic allodynia, but had minimal effect on punctate allodynia. (4) Exogenous BDNF application reversed the suppressive effect of microglial inhibitors on SNI-induced mKCC2 downregulation as well as dynamic allodynia.

Neuropathic pain is initiated or caused by a primary lesion or dysfunction of the nervous system.[21] An SNI model was established to induce neuropathic pain behaviors, including punctate and dynamic allodynia.[13] Previous studies revealed that KCC2 is one of the important mechanisms that mediate punctate allodynia; however, the precise mechanism underlying dynamic allodynia is not clearly understood and effective therapy is still

being explored. In this study, an SNI animal model was established to induce punctate and dynamic allodynia. WB revealed that mKCC2 in the spinal dorsal horn on the injured side of the SNI model was significantly downregulated.[5] Therefore, a connection was speculated to exist between KCC2 expression and dynamic allodynia. Previously, our laboratory studies revealed that Fur, a KCC2 inhibitor—which is also used as a potent loop diuretic to treat edematous states associated with cardiac, renal, and hepatic failure, and hypertension—could stabilize mKCC2 and prevent the usual downregulation of KCC2 during convulsant stimulation in hippocampal neurons. The stabilization of mKCC2 may rapidly recover KCC2 function, enhance GABA receptor efficiency after seizure stimulation, and impede progression from acute seizures to epileptogenesis.[22] In addition, it has been documented that Fur rapidly and reversibly inhibits KCC2 by binding to its large extracellular loop (LEL).[23,24] However, the precise LEL binding site for Fur is unknown. The conserved cysteine residues C287, C302, C322, and C331 in LEL play important roles in KCC2 function. Substitution of any of these residues abolishes KCC2 transport activity but does not alter KCC2 expression.[25,26] Therefore, Fur might suppress KCC2 function while maintaining mKCC2 expression by binding and blocking one or more of the aforementioned cysteine residues.[15,22] Therefore, Fur was intrathecally injected 30 min after surgery to prevent mKCC2 downregulation in the current study after SNI injury. Although the exact mechanism of action of Fur is not fully understood, it is believed to act on the luminal surface of the ascending limb of Henle by inhibiting the active reabsorption of chloride.[27] In our current study, we hypothesized that Fur was by binding to the mKCC2 surface to physically interact with the mKCC2 protein to block mKCC2 internalization for preventing its downregulation. However, this mechanism needs to be further investigated. Nevertheless, we observed that Fur treatment did indeed block SNI-induced mKCC2 reduction, thus inhibiting SNI-induced dynamic allodynia. In addition, we chose to administer Fur 30 min after SNI surgery because previous studies found that BDNF-TrkB mediated significant downregulation of KCC2 in 2 hours and reached the lowest level 6 hours after seizure.[28] Furthermore, the downregulation of KCC2 starts as early as excitatory stimulation occurring immediately after injury.[29] We aimed to prevent the obvious downregulation of KCC2 by intervention at an early stage after SNI in this study.

Microglia in the spinal dorsal horn are activated after peripheral nerve injury, and activation of the microglia is associated with the P2X4 receptor. Therefore, Mino (30 nmol), a tetracycline derivative reported to suppress hypoxic activation of cultured microglia by inhibiting the p38 mitogen-activated protein kinase pathway,[17] was used to inhibit microglial activation within half an hour after the SNI model establishment.[30] In our current study, the behavioral findings revealed that Mino had no effect on punctate allodynia induced in the SNI model; however, a temporary relief effect was observed on the first and second days after the operation for dynamic allodynia. This effect may be due to the induction of punctate and dynamic allodynia via different transduction pathways. Many previous studies have shown that the mechanisms responsible for these two types of allodynia are different.[31–33] Punctate allodynia is sensitive to morphine, whereas the dynamic allodynia is insensitive to morphine analgesia.[32] The relief effect on dynamic allodynia lasted only 2 days, which may be related to the half-life of Mino, aligning the results of previous studies in our laboratory.[10] Both WB and immunohistochemical results showed that SNI-induced KCC2 downregulation was reversed in SNI mice treated with Mino (30 nmol), while microglial activation was mostly inhibited. Overall, our results demonstrated that the inhibition of microglial activation can inhibit KCC2 downregulation and dynamic allodynia. Previously, Mino (30 mg/kg, i.p.) was injected 1 h before or 7 days after nerve injury, and continuously administered until day 14 in the preemptive or postinjury part of the study, respectively. In a preventive study, Mino increased the expression of KCC2 and GABA-A/r2 proteins, and decreased BDNF expression. In contrast, target gene and protein expression did not change when Mino was administered after nerve injury.[34] Accordingly, the mechanism identified here could act prior to neuropathic pain. Following SNI, adenosine triphosphate is released to act on the P2X4 receptor in microglia, resulting in neuropathic pain.[35] Based on abundant evidence, ionic ATP signaling promotes pain mechanisms in physiological and pathological environments through the involvement of P2X3, P2X4, and P2X7 ATP receptors. Studies have revealed that after nerve injury, the expression of P2X4Rs in the spinal cord is upregulated exclusively in microglia, but not in neurons or astrocytes.[36] P2X4Rs are ATP-gated channels with a high calcium permeability. Accumulating evidence suggests that P2X4Rs are expressed in the central microglia and peripheral macrophages. In peripheral inflammatory responses, the activation of P2X4Rs evokes calcium influx and p38-MAPK phosphorylation, resulting in the release of prostaglandin E2 (PGE2).[37] However, in microglia, P2X4Rs mainly cause the release of BDNF, a key molecule for maintaining pain hypersensitivity after nerve injury. 5BDBD, a specific P2X4R antagonist, was selected for intrathecal injection. Based on previous results, 5BDBD can be used to study the endogenous role of P2X4R in the central nervous system, and the antagonist can distinguish between P2X4R and others when co-expressed in the same tissue.[35] Behavioral findings showed that 5BDBD had a temporary relief effect on punctate allodynia caused by SNI 1 day after surgery, and dynamic allodynia was significantly reduced in the treatment group compared to that in the SNI group. WB results also revealed that KCC2 downregulation

was reversed after treatment with the P2X4R blocker 5BDBD. The immunofluorescence results showed that 5BDBD significantly inhibited microglial activation in the spinal dorsal horn on the injured side. In conclusion, inhibition of microglia activation can inhibit KCC2 downregulation and dynamic allodynia.

Finally, microglial activation was shown to lead to the downregulation of KCC2 through the BDNF-TrkB pathway. BDNF is a crucial neuromodulator in pain transmission in the peripheral and central nervous systems, and microglia in the nervous system are one of the major sources of BDNF release.[38] Previous studies have shown that BDNF-TrkB signaling modulates the pain process by regulating neuroinflammation, which has also been reported in other pathological pain models.[39] Furthermore, the BDNF-TrkB pathway can affect the pathological development and functional improvement of spinal cord injuries.[40,41] We surmise that peripheral nerve injuries elicit BDNF release to activate TrkB receptors in the spinal dorsal horn. The activation of these receptors mediates some of the early consequences of injury-elicited plasticity, including the downregulation of neuronal mKCC2. Based on our results, early behavioral signs of pain could be effectively attenuated by a single pre-treatment with the nonspecific tyrosine kinase blocker, K252a. A similar effective analgesic action of K252a was previously reported in a study of cyclophosphamide-elicited mechanical allodynia of the bladder.[42] Immunohistochemistry and WB showed that KCC2 downregulation was qualitatively and quantitatively reversed by TrkB inhibition owing to K252a treatment in the spinal dorsal horn. These results suggest that microglial activation leads to KCC2 downregulation through the BDNF-TrkB pathway, resulting in dynamic allodynia. Previously, intrathecal injection of exogenous BDNF in animal models of cystitis was reported to further promote the activation of astrocytes and microglia, aggravate neuroinflammation, and aggravate mechanical ectopic pain.[43] The intrathecal injection of a high dose of exogenous BDNF (3 ng/10 μL) in the sham operation group was found to significantly cause punctate and dynamic allodynia, and immunohistochemistry and WB revealed that the intrathecal injection of a high dose of exogenous BDNF in the sham operation group could significantly lead to the downregulation of KCC2. Such findings indicate that the activation of the BDNF-TrkB pathway leads to the downregulation of KCC2 and mechanical allodynia. Furthermore, the intrathecal injection of exogenous BDNF, in addition to Mino to block microglia activation after SNI surgery, revealed that the inhibition of dynamic allodynia by the microglia inhibitor was significantly reversed by BDNF, which correlated with the prevention of mKCC2 downregulation.

Many studies have shown that GABA inhibition is critically dependent on KCC2 activity, and the loss of this activity may lead to reduced GABA inhibition in the dorsal horn neuronal circuit.[36] In fact, various neuropathic pain models have demonstrated a decrease in KCC2 expression in the spinal cord. The alteration of KCC2 expression affects GABAergic and glycinergic neurotransmission, as KCC2 is a chloride cotransporter that serves to maintain intracellular chloride concentration. We assume that at any given time, a balance between excitatory and inhibitory processes determines the degree of overall neuronal excitability in the dorsal horn, and the loss of GABA inhibition tips the balance toward excitation. This increased excitability then sustains enhanced (and exaggerated) communication between the primary afferents and dorsal horn neurons, contributing to early behavioral signs of pain. This is consistent with the behavioral results of dynamic allodynia caused by KCC2 downregulation in the spinal dorsal horn.

To our knowledge, this is the first study to reveal that SNI induces the downregulation of mKCC2 contributing to dynamic allodynia, but had less effect on punctate allodynia. Furthermore, dynamic allodynia is closely related to the downregulation of mKCC2 through the activation of the BDNF-TrkB pathway after SNI-induced activation of the microglia in the spinal dorsal horn. Our findings provide new insights into the mechanism of dynamic allodynia, distinguishing it from punctate allodynia in the neuronal circuit of the spinal dorsal horn, ultimately revealing a new therapeutic target specifically for the treatment of dynamic allodynia.

Author contributions

XZ, TZ, YW conceived the study design. ZH, XY, TZ, PC, GW established the animal model, performed the pain behavior study. ZH, PC, JZ, JY prepared the brain tissues, performed the immunostaining and obtained the confocal pictures. XY, PC, JY, TZ performed western blotting. ZH, XY, JY, and TW analyzed the data. ZH, XY, PC, KY, TZ, YW and XZ wrote, commented and modified the manuscript. All authors approved the final version of the manuscript.

Declaration of conflicting interests

The author(s) declared no potential conflicts of interest with respect to the research, authorship, and/or publication of this article.

Funding

The author(s) disclosed receipt of the following financial support for the research, authorship, and/or publication of this article: This work was funded by NSFC grants (81873787, 32111530119 and 31771188), and supported by Shanghai Municipal Science and Technology Major Project (No.2018SHZDZX01), ZJ Lab, and Shanghai Center for Brain Science and Brain-Inspired Technology. It also supported by a grant from Natural Science Foundation of Shanghai [No. 18ZR1424800] to XZ and a grant from the Sanming Project of Medicine in Shenzhen (No. SZSM202111010) to YW. Xuan Zhao (81873787).

ORCID iDs

Fuqing Lin https://orcid.org/0000-0002-6478-0013
Xuan Zhao https://orcid.org/0000-0003-4018-0360

References

1. Cavalli E, Mammana S, Nicoletti F, Bramanti P, Mazzon E. The neuropathic pain: an overview of the current treatment and future therapeutic approaches. *Int J Immunopathol Pharmacol* 2019; 33: 1–10. DOI: 10.1177/2058738419838383.
2. Petitjean H, Pawlowski SA, Fraine SL, Sharif B, Hamad D, Fatima T, Berg J, Brown CM, Jan LY, Ribeiro-da-Silva A, Braz JM, Basbaum AI, Sharif-Naeini R. Dorsal horn parvalbumin neurons are gate-keepers of touch-evoked pain after nerve injury. *Cell Rep* 2015; 13: 1246–1257. DOI: 10.1016/j.celrep.2015.09.080
3. Jensen TS, Finnerup NB. Allodynia and hyperalgesia in neuropathic pain: clinical manifestations and mechanisms. *Lancet Neurol* 2014; 13: 924–935. DOI: 10.1016/s1474-4422(14)70102-4.
4. Koltzenburg M, Lundberg LER, Torebjörk HE. Dynamic and static components of mechanical hyperalgesia in human hairy skin. *Pain* 1992; 51: 207–219. DOI: 10.1016/0304-3959(92)90262-a
5. Kitayama T. The Role of K(+)-Cl(-)-Cotransporter-2 in neuropathic pain. *Neurochem Res* 2018; 43: 110–115. DOI: 10.1007/s11064-017-2344-3.
6. Sucena E, Delon I, Jones I, Payre F, Stern DL. Regulatory evolution of shavenbaby/ovo underlies multiple cases of morphological parallelism. *Nature* 2003; 424: 935–938. DOI: 10.1038/nature01768.
7. Jolivalt CG, Lee CA, Ramos KM, Calcutt NA. Allodynia and hyperalgesia in diabetic rats are mediated by GABA and depletion of spinal potassium-chloride co-transporters. *Pain* 2008; 140: 48–57. DOI: 10.1016/j.pain.2008.07.005.
8. Chen Y, Shi Y, Wang G, Li Y, Cheng L, Wang Y. Memantine selectively prevented the induction of dynamic allodynia by blocking Kir2.1 channel and inhibiting the activation of microglia in spinal dorsal horn of mice in spared nerve injury model. *Mol Pain* 2019; 15: 1–11. DOI: 10.1177/1744806919838947.
9. Coull JA, Beggs S, Boudreau D, Boivin D, Tsuda M, Inoue K, Gravel C, Salter MW, De Koninck Y. BDNF from microglia causes the shift in neuronal anion gradient underlying neuropathic pain. *Nature* 2005; 438: 1017–1021. DOI: 10.1038/nature04223.
10. Cheng L, Duan B, Huang T, Zhang Y, Chen Y, Britz O, Garcia-Campmany L, Ren X, Vong L, Lowell BB, Goulding M, Wang Y, Ma Q. Identification of spinal circuits involved in touch-evoked dynamic mechanical pain. *Nat Neurosci* 2017; 20: 804–814. DOI: 10.1038/nn.4549.
11. Shi Y, Chen Y, Wang Y. Kir2.1 channel regulation of glycinergic transmission selectively contributes to dynamic mechanical allodynia in a mouse model of spared nerve injury. *Neurosci Bull* 2019; 35: 301–314. DOI: 10.1007/s12264-018-0285-8.
12. Li W, Cai J, Wang BH, Huang L, Fan J, Wang Y. Antinociceptive effects of novel epibatidine analogs through activation of α4β2 nicotinic receptors. *Sci China Life Sci* 2018; 61: 688–695. DOI: 10.1007/s11427-017-9062-3.
13. Duan B, Cheng L, Bourane S, Britz O, Padilla C, Garcia-Campmany L, Krashes M, Knowlton W, Velasquez T, Ren X, Ross S, Lowell BB, Wang Y, Goulding M, Ma Q. Identification of spinal circuits transmitting and gating mechanical pain. *Cell* 2014; 159: 1417–1432. DOI: 10.1016/j.cell.2014.11.003.
14. Howard RF, Walker SM, Mota PM, Fitzgerald M. The ontogeny of neuropathic pain: Postnatal onset of mechanical allodynia in rat spared nerve injury (SNI) and chronic constriction injury (CCI) models. *Pain* 2005; 115: 382–389. DOI: 10.1016/j.pain.2005.03.016
15. Wan L, Chen L, Yu J, Wang G, Wu Z, Qian B, Liu X, Wang Y. Coordinated downregulation of KCC2 and GABA(A) receptor contributes to inhibitory dysfunction during seizure induction. *Biochem Biophys Res Commun* 2020; 532: 489–495. DOI: 10.1016/j.bbrc.2020.08.082
16. Zhao H, Alam A, Chen Q, A Eusman M, Pal A, Eguchi S, Wu L, Ma D. The role of microglia in the pathobiology of neuropathic pain development: what do we know? *Br J Anaesth* 2017; 118: 504–516. DOI: 10.1093/bja/aex006.
17. Suk K. Minocycline suppresses hypoxic activation of rodent microglia in culture. *Neurosci Lett* 2004; 366: 167–171. DOI: 10.1016/j.neulet.2004.05.038.
18. Coddou C, Sandoval R, Hevia MJ, Stojilkovic SS. Characterization of the antagonist actions of 5-BDBD at the rat P2X4 receptor. *Neurosci Lett* 2019; 690: 219–224. DOI: 10.1016/j.neulet.2018.10.047.
19. Lee-Hotta S, Uchiyama Y, Kametaka S. Role of the BDNF-TrkB pathway in KCC2 regulation and rehabilitation following neuronal injury: a mini review. *Neurochem Int* 2019; 128: 32–38. DOI: 10.1016/j.neuint.2019.04.003.
20. Guo D, Hou X, Zhang H, Sun W, Zhu L, Liang J, Jiang X. More expressions of BDNF and TrkB in multiple hepatocellular carcinoma and anti-BDNF or K252a induced apoptosis, supressed invasion of HepG2 and HCCLM3 cells. *J Exp Clin Cancer Res* 2011; 30: 1–8. DOI: 10.1186/1756-9966-30-97.
21. Vote BJ, Newland A, Polkinghorne PJ. Humidity devices in vitreoretinal surgery. *Retina* 2002; 22: 616–621. DOI: 10.1097/00006982-200210000-00013.
22. Chen L, Yu J, Wan L, Wu Z, Wang G, Hu Z, Ren L, Zhou J, Qian B, Zhao X, Zhang J, Liu X, Wang Y. Furosemide prevents membrane KCC2 downregulation during convulsant stimulation in the hippocampus. *IBRO Neurosci Rep* 2022; 12: 355–365. DOI: 10.1016/j.ibneur.2022.04.010
23. Ponto LL, Schoenwald RD. Furosemide (frusemide). A pharmacokinetic/pharmacodynamic review (Part I). *Clin Pharmacokinet* 1990; 18: 381–408. DOI: 10.2165/00003088-199018050-00004.
24. Zhou YQ, Liu DQ, Chen SP, Sun J, Wang XM, Tian YK, Wu W, Ye DW. Minocycline as a promising therapeutic strategy for chronic pain. *Pharmacol Res* 2018; 134: 305–310. DOI: 10.1016/j.phrs.2018.07.002.
25. Ochoa JL, Yarnitsky D. Mechanical hyperalgesias in neuropathic pain patients: dynamic and static subtypes. *Ann Neurol* 1993; 33: 465–472. DOI: 10.1002/ana.410330509.
26. Field MJ, Bramwell S, Hughes J, Singh L. Detection of static and dynamic components of mechanical allodynia in rat models of neuropathic pain: are they signalled by distinct primary sensory

neurones? *Pain* 1999; 83: 303–311. DOI: 10.1016/s0304-3959(99)00111-6.

27. Field MJ, McCleary S, Hughes J, Singh L. Gabapentin and pregabalin, but not morphine and amitriptyline, block both static and dynamic components of mechanical allodynia induced by streptozocin in the rat. *Pain* 1999; 80: 391–398. DOI: 10.1016/s0304-3959(98)00239-5.
28. Zarei M, Sabetkasaei M, Moini Zanjani T, Sahebi Vaighan N. The effect of microglial inhibition on the expression of BDNF, KCC2, and GABAA receptor before and after the establishment of CCI-induced neuropathic pain model. *Fundam Clin Pharmacol* 2022; 36: 277–285. DOI: 10.1111/fcp.12719
29. Bernier LP, Ase AR, Séguéla P. P2X receptor channels in chronic pain pathways. *Br J Pharmacol* 2018; 175: 2219–2230. DOI: 10.1111/bph.13957.
30. Long T, He W, Pan Q, Zhang S, Zhang D, Qin G, Chen L, Zhou J. Microglia P2X4R-BDNF signalling contributes to central sensitization in a recurrent nitroglycerin-induced chronic migraine model. *J Headache Pain* 2020; 21: 4–17. DOI: 10.1186/s10194-019-1070-4.
31. Ulmann L, Hirbec H, Rassendren F. P2X4 receptors mediate PGE2 release by tissue-resident macrophages and initiate inflammatory pain. *Embo J* 2010; 29: 2290–2300. DOI: 10.1038/emboj.2010.126.
32. Cappoli N, Tabolacci E, Aceto P, Dello Russo C. The emerging role of the BDNF-TrkB signaling pathway in the modulation of pain perception. *J Neuroimmunol* 2020; 349: 577406.
33. Luo H, Xiang Y, Qu X, Liu H, Liu C, Li G, Han L, Qin X. Apelin-13 suppresses neuroinflammation against cognitive deficit in a streptozotocin-induced rat model of alzheimer's disease through activation of BDNF-TrkB signaling pathway. *Front Pharmacol* 2019; 10: 395. DOI: 10.3389/fphar.2019.00395
34. Boulenguez P, Liabeuf S, Bos R, Bras H, Jean-Xavier C, Brocard C, Stil A, Darbon P, Cattaert D, Delpire E, Marsala M, Vinay L. Down-regulation of the potassium-chloride cotransporter KCC2 contributes to spasticity after spinal cord injury. *Nat Med* 2010; 16: 302–307. DOI: 10.1038/nm.2107.
35. Rivera C, Voipio J, Thomas-Crusells J, Li H, Emri Z, Sipilä S, Payne JA, Minichiello L, Saarma M, Kaila K. Mechanism of activity-dependent downregulation of the neuron-specific K-Cl cotransporter KCC2. *J Neurosci* 2004; 24: 4683–4691. DOI: 10.1523/jneurosci.5265-03.2004.
36. Guerios SD, Wang ZY, Bjorling DE. Nerve growth factor mediates peripheral mechanical hypersensitivity that accompanies experimental cystitis in mice. *Neurosci Lett* 2006; 392(3): 193–197. DOI: 10.1016/j.neulet.2005.09.026
37. Ding H, Chen J, Su M, Lin Z, Zhan H, Yang F, Li W, Xie J, Huang Y, Liu X, Liu B, Zhou X. BDNF promotes activation of astrocytes and microglia contributing to neuroinflammation and mechanical allodynia in cyclophosphamide-induced cystitis. *J Neuroinflammation* 2020; 17: 1–13. DOI: 10.1186/s12974-020-1704-0.
38. Watanabe M, Zhang J, Mansuri MS, Duan J, Karimy JK, Delpire E, Alper SL, Lifton RP, Fukuda A, Kahle KT. Developmentally regulated KCC2 phosphorylation is essential for dynamic GABA-mediated inhibition and survival. *Sci Signal* 2019; 12: eaaw9315. DOI: 10.1126/scisignal.aaw9315.
39. Luo H, Xiang Y, Qu X, Liu H, Liu C, Li G, Han L, Qin X. Apelin-13 Suppresses Neuroinflammation Against Cognitive Deficit in a Streptozotocin-Induced Rat Model of Alzheimer's Disease Through Activation of BDNF-TrkB Signaling Pathway. *Frontiers in pharmacology* 2019; 10: 395. DOI: 10.3389/fphar.2019.00395.
40. Boulenguez P, Liabeuf S, Bos R, Bras H, Jean-Xavier C, Brocard C, Stil A, Darbon P, Cattaert D, Delpire E, Marsala M, Vinay L. Down-regulation of the potassium-chloride cotransporter KCC2 contributes to spasticity after spinal cord injury. *Nature medicine* 2010; 16: 302–307. DOI: 10.1038/nm.2107.
41. Rivera C, Voipio J, Thomas-Crusells J, Li H, Emri Z, Sipilä S, Payne JA, Minichiello L, Saarma M, Kaila K. Mechanism of activity-dependent downregulation of the neuron-specific K-Cl cotransporter KCC2. *The Journal of neuroscience: the official journal of the Society for Neuroscience* 2004; 24: 4683–4691. DOI: 10.1523/jneurosci.5265-03.2004.
42. Guerios SD, Wang ZY, Bjorling DE. Nerve growth factor mediates peripheral mechanical hypersensitivity that accompanies experimental cystitis in mice. *Neuroscience letters* 2006; 392: 193–197. DOI: 10.1016/j.neulet.2005.09.026.
43. Ding H, Chen J, Su M, Lin Z, Zhan H, Yang F, Li W, Xie J, Huang Y, Liu X, Liu B, Zhou X. BDNF promotes activation of astrocytes and microglia contributing to neuroinflammation and mechanical allodynia in cyclophosphamide-induced cystitis. *Journal of neuroinflammation* 2020; 17: 19. DOI: 10.1186/s12974-020-1704-0.